European Commission
FP7, Grant Agreement 211143

Role of high-order Laguerre-Gauss modes on mirror thermal noise in gravitational wave detectors

ET-0002A-10

Janyce Franc, Massimo Galimberti, Raffaele Flaminio
Laboratoire des Matériaux Avancés
7 avenue Pierre de Coubertin, 69622 Villeurbanne

Simon Chelkowski, Andreas Freise
School of Physics and Astronomy
University of Birmingham
B15 2TT, UK

Stefan Hild
Institute for Gravitational Research
University of Glasgow
Glasgow, G128QQ, UK

Issue: 1
Date: June 14, 2010

Contents

Abstract

We present a detailed calculation of the impact of high-order Laguerre-Gauss (LG) modes on mirror thermal noise in interferometric gravitational wave detectors (GWD). We take into account configurations with mirrors of finite and infinite size. The size of the mirror can be optimized to decrease thermal noise effect and the beam size is calculated for 1 ppm diffraction losses. These modes have been already proposed for advanced-GWD for their interesting properties with respect to thermal noise and thermal lensing. The rationale of this note is the understanding of the sensitivity behaviour of the detector sensitivity when using high-order LG modes, for different substrate materials and mirror dimensions.

I. INTRODUCTION

The third generation of gravitational wave detectors requires a decrease in sensitivity from 4 10^{-24} to 2 10^{-25} 1/sqrt(Hz) at 100 Hz. Figure 1 represents the fundamental noise budget of advanced detectors (blue line). The dashed curves show the different noise contributions. The main limitation to sensitivity in the range of frequencies going from 50 to 500 Hz comes from the coating Brownian noise (dashed red line) [1]. Several ideas have been proposed in order to decrease thermal noise: cooling mirrors, using new coatings, increasing the length of Fabry-Perot cavities, using a different beam profile, increasing the beam size of the mirror. This note focuses on the use of high-order Laguerre-Gauss (LG) modes; its goal is to evaluate mirror thermal noises when LG modes are used.

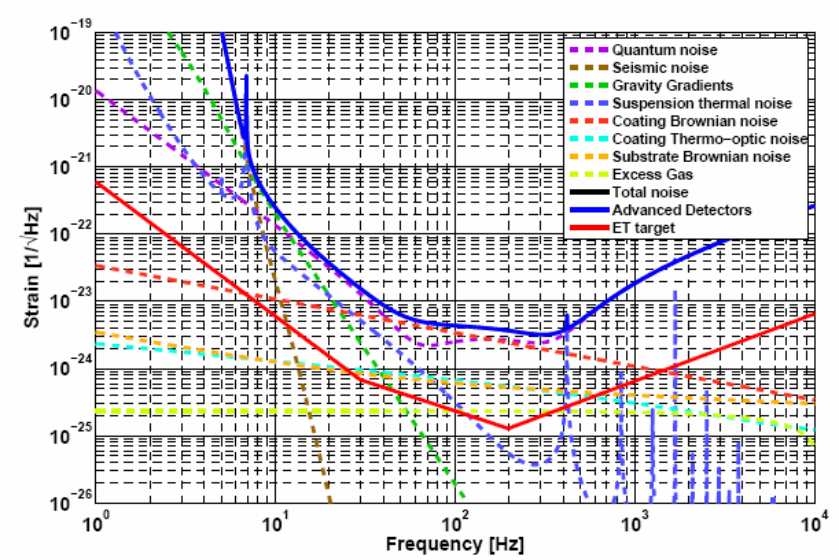

Figure 1 Fundamental noise for advanced detectors (blue line) and target noise curve for ET (red line)

High-order LG modes present several advantages with respect to the fundamental LG_{00} mode in order to improve the sensitivity of advanced detectors. The light intensity is spread more homogeneously over the mirror surface. That allows to decrease the thermal noise [2]. High-order LG modes allow also to decrease the temperature gradients on the mirrors and thus the thermal lensing [3].

This note is specifically devoted to mirror thermal noise. Three different materials and two different temperatures have been considered for mirror substrates: silicon at 10 K, sapphire at 10 K and silica at 300 K. The parameters used for substrate and coating at room and cryogenic temperature are listed in the ET note ET-09021.

II. STATE OF THE ART: LAGUERRE-GAUSS MODES

Laguerre-Gauss modes are a solution to the scalar propagation equation in the paraxial approximation; in contrast to Hermite-Gauss modes, we use the so-called helical Laguerre-Gauss modes with circular symmetry [4]. The modes are denoted $LG_{m,n}$ where m and n are respectively the radial and angular mode orders. The mode $m=n=0$ is the fundamental Gaussian mode; higher-order LG modes can have a ring-shaped or a shamrock-shaped carrier distribution for instance. High-order modes are relatively larger in diameter compared to the fundamental beam: the first advantage of using LG modes is the shape of the beam spreading the power distribution on the mirror surface.
The normalized pressure distribution on the surface of a mirror is proportional to the intensity of the light and has thus the following expression [2]:

$$p_m^{(n)}(r) = \frac{2}{\pi w^2}\frac{m!}{(m+n)!}\exp(-2r^2/w^2)(-2r^2/w^2)^n\left[L_m^{(n)}(-2r^2/w^2)\right]^2$$

where $L_m^{(n)}(x)$ denotes a generalized Laguerre polynomial, and w is the beam radius. $L_m^{(n)}(x)$ are defined by the differential expression:

$$L_m^{(n)}(x) = \frac{x^{-n}e^x}{m!}\frac{dm}{dx^m}(e^{-x}x^{m+n})$$

or explicitly:

$$L_m^{(n)}(x) = (-1)^m\left\{\frac{x^m}{m!} - \frac{(m+n)x^{m-1}}{1!(m-1)!} + \frac{(m+n)(m-1+n)x^{m-2}}{2!(m-2)!} - \ldots + \frac{(m+n)(m-1+n)(m-2+n)\ldots(1+n)}{m!}\right\}$$

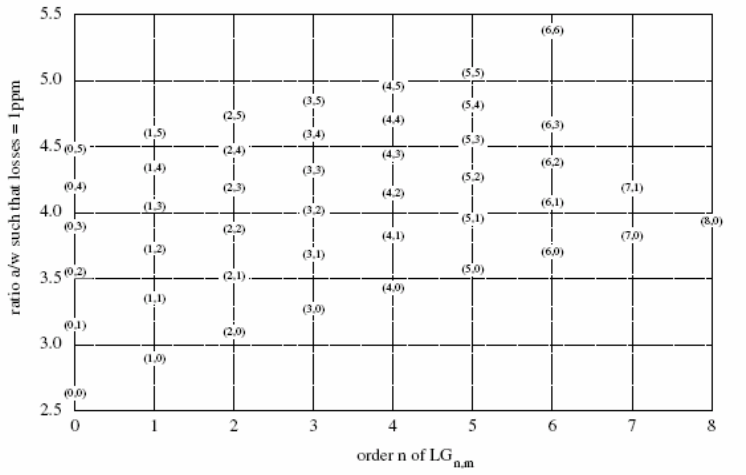

Figure 2 Ratio *a/w* providing 1 ppm diffraction losses versus order of the LG mode

To be assured that diffraction losses stay below 1 ppm, the beam radius *w* must be chosen such that the ratio *a/w* (*a* being the mirror radius) is greater than a threshold. Threshold *a/w* ratios are plotted in figure 2 [2]; their values are 2.6 for $LG_{0,0,}$ 4.3 for $LG_{3,3}$, and 5.1 for $LG_{5,5}$. Beam radii for the different mirror sizes taken into account in this note have been calculated and are listed in table1:

Mirror diameter	Beam radius
35 cm (Virgo and Advanced Virgo)	$w_{0,0}$ = 6.73 cm, $w_{3,3}$ = 4.07 cm, $w_{5,5}$ = 3.43 cm
45 cm (foreseen dimension in 2012 for silicon substrate)	$w_{0,0}$ = 8.65 cm, $w_{3,3}$ = 5.23 cm, $w_{5,5}$ = 4.41 cm
62 cm (optimized diameter for ET baseline design)	$w_{0,0}$ = 11.92 cm, $w_{3,3}$ = 7.21 cm, $w_{5,5}$ = 6.08 cm

Table 1 Maximum beam radii for different mirror diameters, in order to have diffraction losses less than 1 ppm

Figure 3 shows a comparison of the pressure profile of $LG_{0,0}$, $LG_{3,3}$ and $LG_{5,5}$. Again, note that, given the same diffraction losses, high-order LG modes intensity profiles are more uniformly distributed over the mirror surface than the fundamental mode.

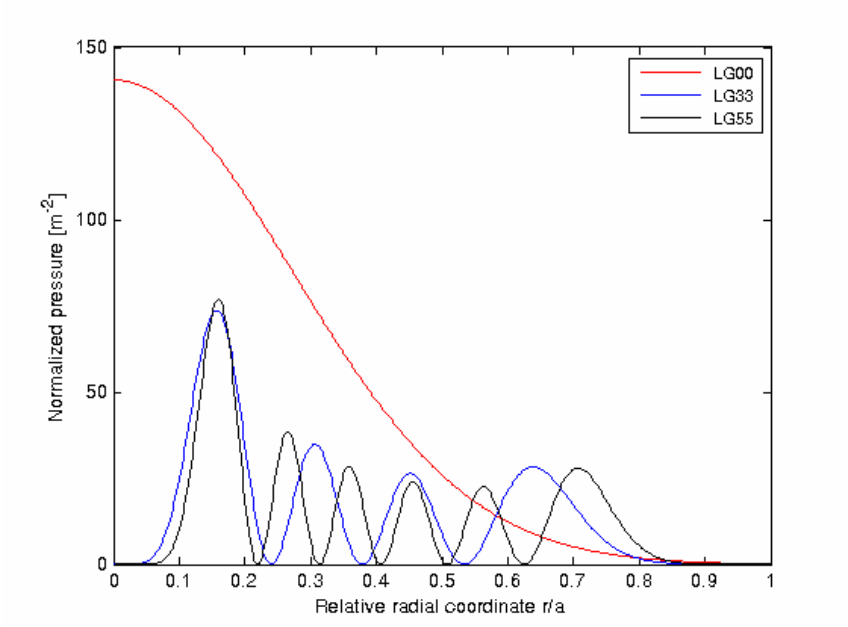

Figure 3 Pressure profiles of Laguerre-Gauss modes

III. DIFFERENT THERMAL NOISE CONTRIBUTIONS WITH LAGUERRE-GAUSS MODES

Four thermal noises contributions will be discussed in this chapter: coating Brownian noise, substrate Brownian noise, coating thermo-elastic noise and substrate thermo-elastic noise. For each noise contribution, two analyses will be presented: first, a comparison of the noise effects of the fundamental mode against the high-order modes as a function of the mirror size, for a fixed substrate (silicon). This will allow to compute the noise reduction factors for the high-order modes. Second, a comparison of different substrates for a fixed mirror size (35 x 20 cm) is presented.

1. Coating Brownian noise
    i. Mirror dimensions (silicon at 10K)

Mirror dimensions induce some significant differences when comparing $LG_{0,0}$, $LG_{3,3}$ and $LG_{5,5}$. The computations have been done for finite and infinite mirrors following the formula given by [5]. Infinite mirrors are used as a reference case. For finite mirrors, the following sizes have been considered.

a) a diameter of 35 cm and a thickness of 10 cm, corresponding to the Virgo design

b) a diameter of 35 cm and a thickness of 20 cm, corresponding to the Advanced Virgo design

c) a diameter of 45 cm and a thickness of 30 cm which is a plausible configuration for the future Einstein Telescope

d) a diameter of 62 cm and a thickness of 30 cm, that is the configuration presented in [6].

These 4 sizes will be used all throughout the present section.

Figure 4 shows the computed coating Brownian noise for the four cases. The coating is a standard thin-film stack of low refractive index SiO_2 and high refractive index $Ti:Ta_2O_5$. The loss angles taken into account for these two materials are respectively, $0.5\ 10^{-4}$ and $2\ 10^{-4}$ for each cases. The configuration of the coating is $(HL)_{19}HLL$ (H stands for high refractive index thin film and L for low refractive index thin film). 19 doublets of thin films on silicon substrate illuminated with a wavelength of 1550 nm (silicon is transparent for wavelength > 1500 nm) correspond to a transmission of 6 ppm.

Ø = 35 cm and h=10 cm

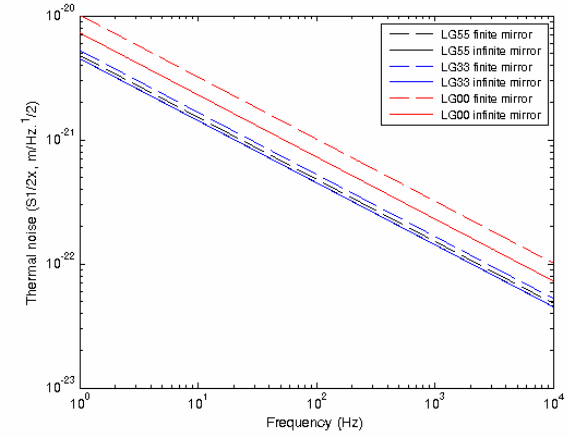

Ø = 35 cm and h=20 cm

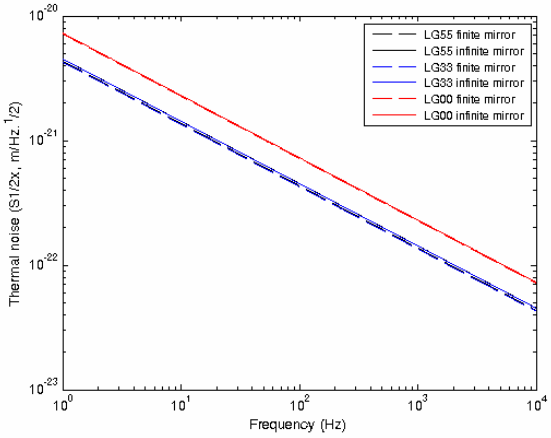

Ø = 45 cm and h=30 cm

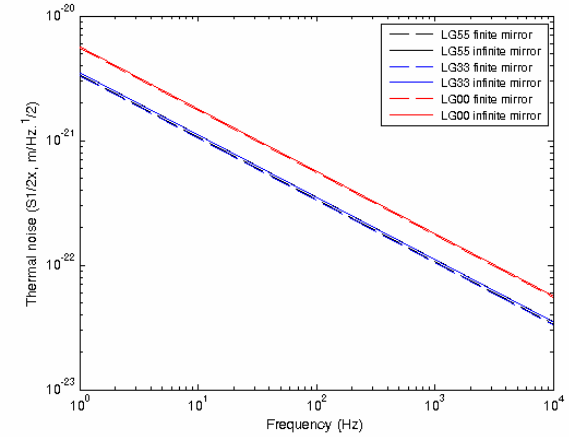

Ø = 62 cm and h=30 cm

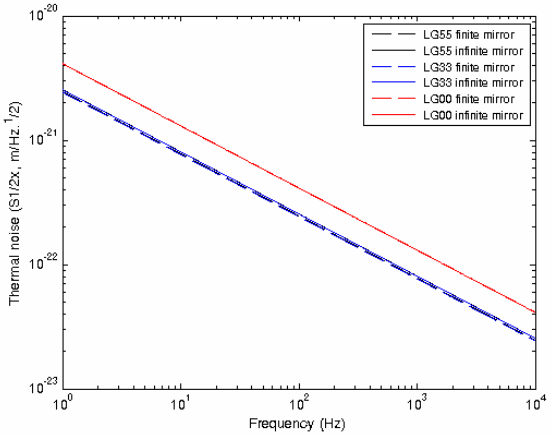

Figure 4 Coating Brownian noise spectral density between 1 Hz and 10 kHz for different mirror sizes and different beam shapes

		Ø = 35 cm h = 10 cm		Ø = 35 cm h = 20 cm		Ø = 45 cm h = 30 cm		Ø = 62 cm h = 30 cm	
	Beam	w (cm)	Sx (10^{-21} m/√Hz)	w (cm)	Sx (10^{-21} m/√Hz)	w (cm)	Sx (10^{-21} m/√Hz)	w (cm)	Sx (10^{-21} m/√Hz)
Finite mirror	$LG_{0,0}$	6.7	10.2	6.7	7.20	8.6	5.56	11.9	4.15
	$LG_{3,3}$	4.1	5.29	4.1	4.27	5.2	3.32	7.2	2.43
	$LG_{5,5}$	3.4	4.83	3.4	4.36	4.4	3.38	6.1	2.47
Infinite mirror	$LG_{0,0}$	6.7	7.32	6.7	7.32	8.6	5.70	11.9	4.13
	$LG_{3,3}$	4.1	4.53	4.1	4.53	5.2	3.52	7.2	2.56
	$LG_{5,5}$	3.4	4.54	3.4	4.54	4.4	3.53	6.1	2.56

Table 2 Coating Brownian noise spectral density value at 1 Hz for all configurations

Table 2 presents the value of the noise spectral density at 1 Hz for each case. From the plots and the table it can easily be seen that high-order LG modes result in smaller coating Brownian noise compared to the results obtained with a fundamental mode. There is no significant difference between $LG_{3,3}$ and $LG_{5,5}$ for an infinite mirror, whereas for a finite mirror $LG_{3,3}$ brings in a noise contribution smaller of about 2% with respect to $LG_{5,5}$ (except for case (a)).

In general, thermal noise decreases when the diameter of the mirror and accordingly the size of the beam increase. Moreover, the thermal noise decreases also when the thickness of the mirror increases [7]. As for the thickness, cases (a) and (b) show that it plays a key role in thermal noise value. For a finite mirror, increasing the thickness from 10 cm (a) to 20 cm (b) allows to reduce the thermal noise by a factor 1.4 for $LG_{0,0}$, 1.23 for $LG_{3,3}$, and 1.1 for $LG_{5,5}$. However, it should be noted that for a thickness greater than 10 cm, the coating Brownian noise does not change significantly for a finite or an infinite mirror.

Noise reduction factors are listed in table 3. Since $LG_{3,3}$ and $LG_{5,5}$ have approximately the same noises, only the ratio $LG_{0,0}/LG_{3,3}$ is reported. On the other hand, for a finite mirror, the dependence on the mirror thickness should be noted: when the thickness is 10 cm, the reduction factor is much higher than in the other cases.

	Ø = 35 cm h = 10 cm	Ø = 35 cm h = 20 cm	Ø = 45 cm h = 30 cm	Ø = 62 cm h = 30 cm
$LG_{0,0}/LG_{3,3}$ finite mirror	**1.93**	**1.69**	**1.67**	**1.71**
$LG_{0,0}/LG_{3,3}$ infinite mirror	**1.61**	**1.61**	**1.62**	**1.61**

Table 3 List of the coating Brownian noise reduction factor LG0,0/LG3,3 for finite and infinite mirror according to the mirror dimension

ii. Comparison of substrates

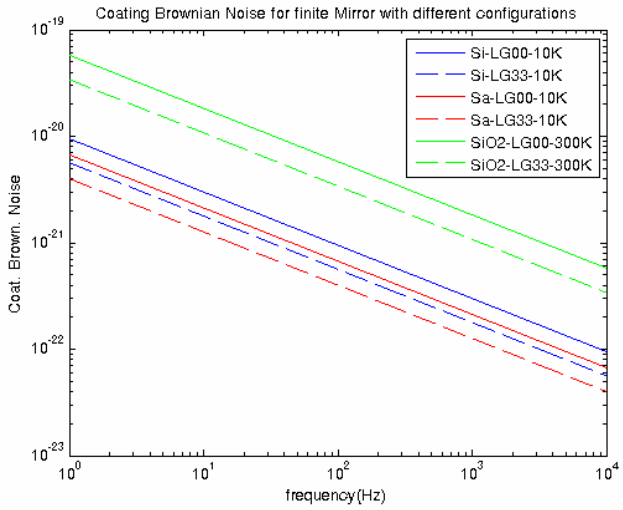

Figure 5 Comparison of coating Brownian noises for a fundamental and a $LG_{3,3}$ beam for three different substrates (silica @ 300K, sapphire @ 10K and silicon @ 10K). Mirror size: diameter 35 cm, thickness 20 cm.

Figure 5 shows the coating Brownian noise for a $LG_{0,0}$ beam and a $LG_{3,3}$ beam. $LG_{5,5}$ has not been plotted because it has been assumed (see figure 4) that the data are not very different, and not necessarily better. Three different substrates have been studied: silica at 300 K, sapphire at 10 K and silicon at 10 K. Silica is the material used in all present GWD (GEO 600, Virgo, LIGO) and is believed to remain the best materials for detectors running at room temperature. Sapphire has been largely studied for the Japanese cryogenic detector LCGT [8]. Finally, silicon can be an alternative to sapphire substrate at low temperature. Several studies have already proved its good optical and mechanical performances [9]. However, silicon is transparent at higher wavelengths (λ=1500 nm) which requires to consider new coating configuration on the mirror surface to perform the prescribed reflectance. The mechanical

losses for SiO_2 and $TiTa_2O_5$ at 300 K and 10 K are respectively 0.5 10^{-4} and 2 10^{-4}. In general, the loss angles at low temperature are higher, but it has been assumed here that these values will be attained when Einstein Telescope is built. Computations have been done for a finite mirror of 35 cm diameter and 20 cm thickness (case (b)). The curves in figure 5 show that the higher LG mode is a good candidate to decrease coating thermal noise in all cases. The best sensitivity is reached when using sapphire.

2. Substrate Brownian noise

   i. Mirror dimensions (silicon at 10K)

Ø = 35 cm and h=10 cm

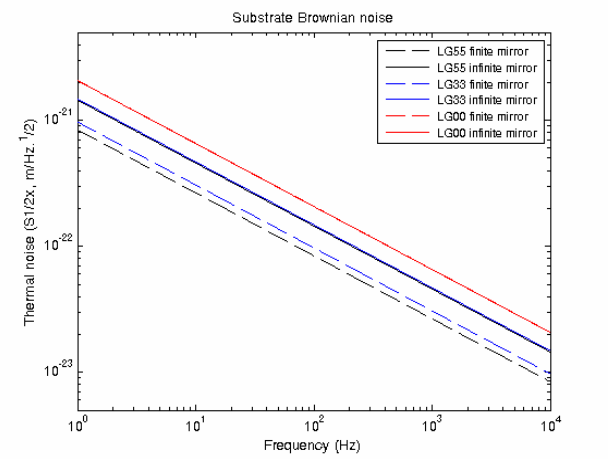

Ø = 35 cm and h=20 cm

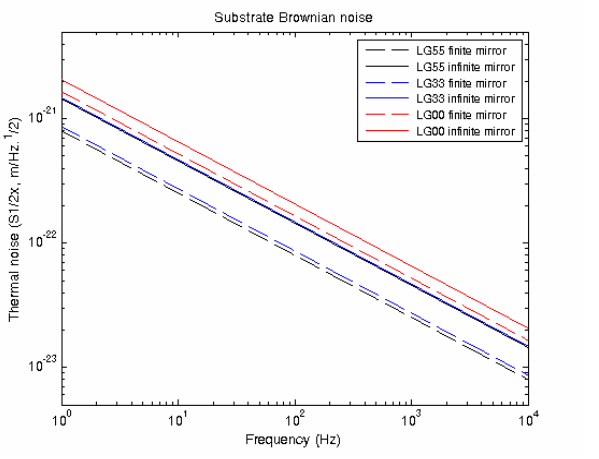

Ø = 45 cm and h=30 cm

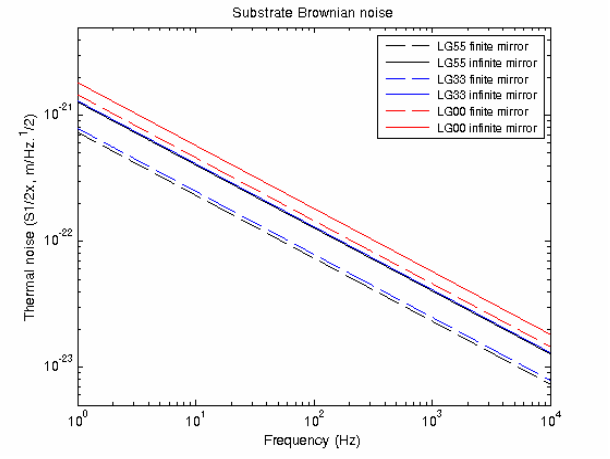

Ø = 62 cm and h=30 cm

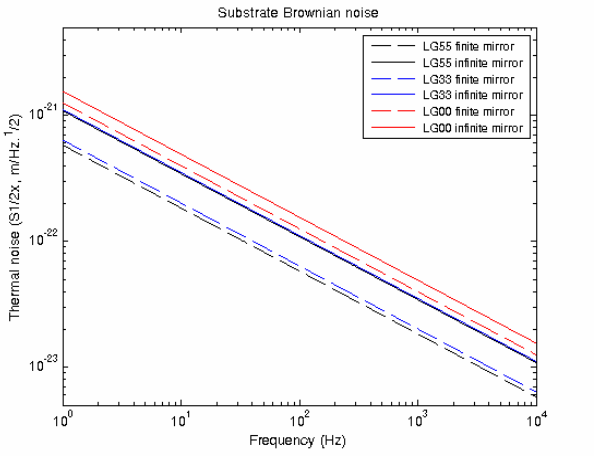

Figure 6 Substrate Brownian noise spectral density between 1Hz and 10 kHz for different mirror sizes and different beam shapes.

Figure 6 shows substrate Brownian noise spectral density for different mirror sizes [5]. It puts in evidence different trends when compared to coating Brownian noise. Concerning the beam profile, high-order LG modes decrease the substrate Brownian noise. $LG_{5,5}$ performs better than $LG_{3,3}$ for a finite mirror. For an infinite mirror there is no significant difference between $LG_{3,3}$ and $LG_{5,5}$. Concerning the mirror dimensions, in general, a finite mirror performs better than an infinite mirror.

		Ø = 35 cm h = 10 cm		Ø = 35 cm h = 20 cm		Ø = 45 cm h = 30 cm		Ø = 62 cm h = 30 cm	
	Beam	w (cm)	Sx (10^{-21} m/√Hz)	w (cm)	Sx (10^{-21} m/√Hz)	w (cm)	Sx (10^{-21} m/√Hz)	w (cm)	Sx (10^{-21} m/√Hz)
Finite mirror	$LG_{0,0}$	6.7	2.09	6.7	1.66	8.6	1.47	11.9	1.26
	$LG_{3,3}$	4.1	0.98	4.1	0.87	5.2	0.78	7.2	0.64
	$LG_{5,5}$	3.4	0.84	3.4	0.80	4.4	0.74	6.1	0.58
Infinite mirror	$LG_{0,0}$	6.7	2.07	6.7	2.07	8.6	1.83	11.9	1.56
	$LG_{3,3}$	4.1	1.49	4.1	1.49	5.2	1.31	7.2	1.12
	$LG_{5,5}$	3.4	1.45	3.4	1.45	4.4	1.28	6.1	1.09

Table 4 Substrate Brownian noise spectral density values at 1 Hz for all configurations

The reduction factor (the ratio $LG_{0,0}/LG_{3,3}$) is shown in table 5. For an infinite mirror the reduction factor is approximately 1.4 for each case independently on thickness. For case (a) the ratio is slightly higher than for the three other cases. In general, high-order modes bring a significant reduction in substrate Brownian noise.

	Ø = 35 cm h = 10 cm	Ø = 35 cm h = 20 cm	Ø = 45 cm h = 30 cm	Ø = 62 cm h = 30 cm
$LG_{0,0}/LG_{3,3}$ finite mirror	**2.13**	**1.90**	**1.88**	**1.97**
$LG_{0,0}/LG_{3,3}$ infinite mirror	**1.39**	**1.39**	**1.40**	**1.39**

Table 5 Substrate Brownian noise reduction factor $LG_{0,0}/LG_{3,3}$ for finite and infinite mirror according to the mirror dimensions

ii. Comparison of substrates

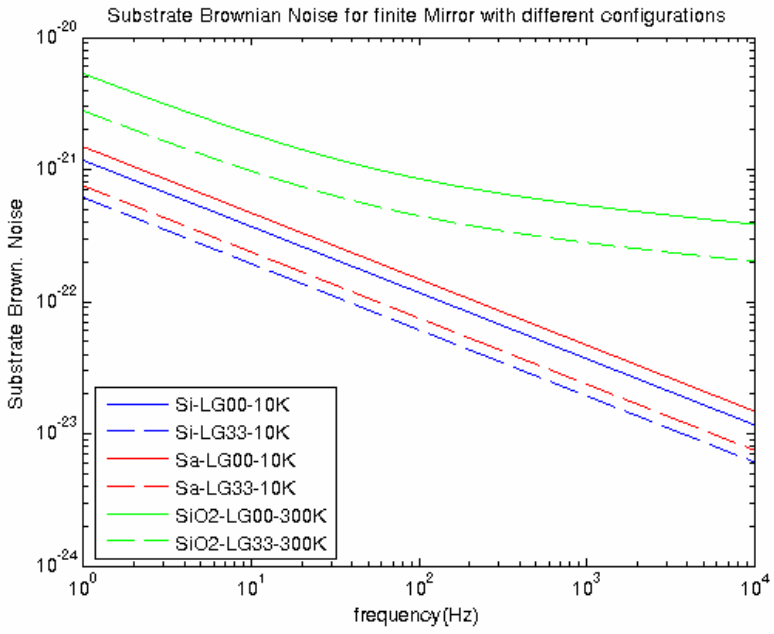

Figure 7 Comparison of substrate Brownian noises for a fundamental and a $LG_{3,3}$ beam for three different substrates (silica @ 300K, sapphire @ 10K and silicon @ 10K). Mirror size: diameter 35 cm, thickness 20 cm.

Figure 7 plots the substrate Brownian noise for a finite mirror with dimensions: diameter 35 cm, thickness 20 cm (case (b)). The mechanical loss angles used for simulations for silica substrate at 300K are calculated from [10] where the mechanical losses are dependent on frequency and surface-to-volume ratio. The calculations are described in [10]

and have been done for fit coefficient of a Suprasil 312 substrate. The mechanical losses of the sapphire substrate at 10 K and the silicon substrate at 10 K are respectively 4 10^{-9} and 1 10^{-9}. The curves show that high-order LG modes perform better for all materials. The best sensitivity is obtained for the silicon substrate.

3. Thermo-elastic coating noise

Thermo-elastic coating noise has not been studied here; the formula presented in [5] are currently under investigation. However, since thermo-elastic coating noise is believed to not be a dominant noise, the authors believe that the conclusions of this note will not change when its contribution is taken into account.

4. Thermo-elastic substrate noise

   i. Mirror dimension (silicon at 10K)

Ø = 35 cm and h=10 cm

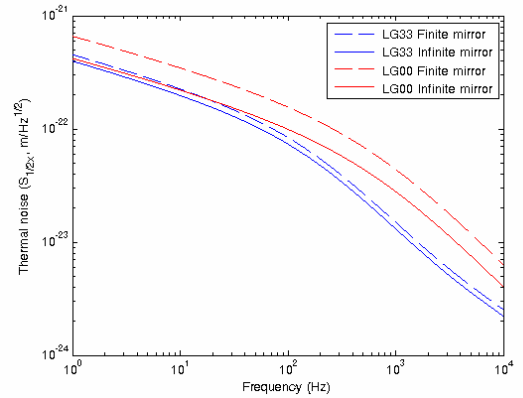

Ø = 35 cm and h=20 cm

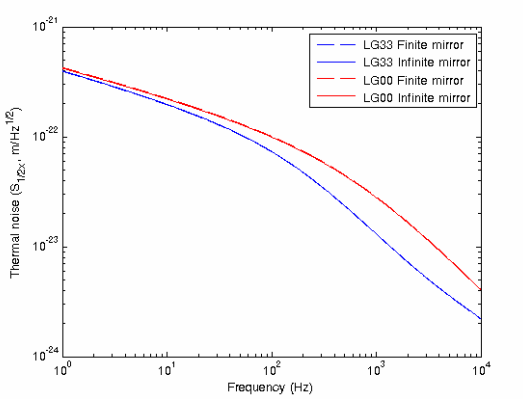

Ø = 45 cm and h=30 cm

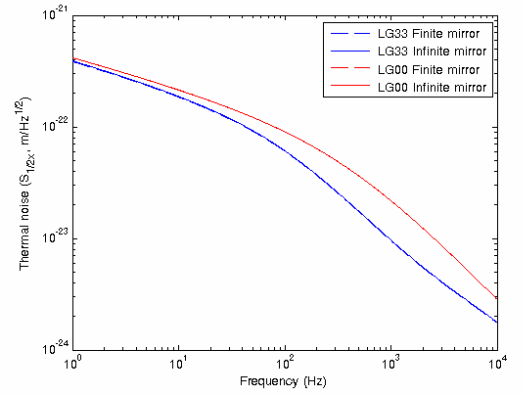

Ø = 62 cm and h=30 cm

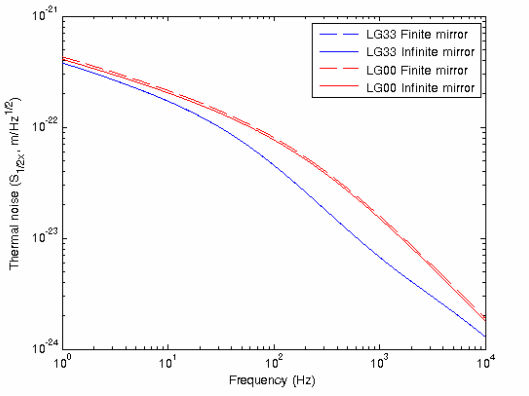

Figure 8 Spectral density of substrate thermo-elastic noise from 1Hz to 10 kHz for different mirror configurations and different beam shapes

Figure 8 shows the thermo-elastic substrate noise for different silicon mirror dimensions of a silicon mirror at 10K. At low temperature, the adiabatic assumption (generally assumed in the thermo-elastic noise formula [11]) fails below an angular frequency [12]. The formula announced by [11] has been only done for a Gaussian beam and no other documents have been listed on the subject. In order to compensate for beam shape, the substrate thermo-elastic noise for higher LG modes without adiabatic assumption has been calculated.

Figure 8 shows that for a thick mirror (>20 cm), there are no significant differences between the noise spectral density of a finite and an infinite mirror. The infinite mirror approximation is thus well adapted. Thin mirrors (<20 cm), on the other hand, are not well approximated by infinite mirrors. For all configuration the $LG_{3,3}$ beam gives the best results. The values of the spectral density and of the reduction factors at 1 Hz are listed in tables 6 and 7.

		Ø : 35 cm h : 10 cm		Ø : 35 cm h : 20 cm		Ø : 45 cm h : 30 cm		Ø : 62 cm h : 30 cm	
	Beam	w (cm)	Sx (10^{-22})	w (cm)	Sx (10^{-22})	w (cm)	Sx (10^{-22})	w (cm)	Sx (10^{-22})
Finite mirror	$LG_{0,0}$	6.7	6.61	6.7	4.28	8.6	4.17	11.9	4.32
	$LG_{3,3}$	4.1	4.55	4.1	3.94	5.2	3.85	7.2	3.80
	$LG_{5,5}$								
Infinite mirror	$LG_{0,0}$	6.7	4.20	6.7	4.21	8.6	4.17	11.9	4.10
	$LG_{3,3}$	4.1	3.98	4.1	3.98	5.2	3.92	7.2	3.80
	$LG_{5,5}$								

Table 6 Spectral density of substrate thermo-elastic noise at 1 Hz for all configurations

	Ø = 35 cm h = 10 cm	Ø = 35 cm h = 20 cm	Ø = 45 cm h = 30 cm	Ø = 62 cm h = 30 cm
$LG_{0,0}/LG_{3,3}$ finite mirror	**1.45**	**1.09**	**1.08**	**1.13**
$LG_{0,0}/LG_{3,3}$ infinite mirror	**1.06**	**1.06**	**1.06**	**1.08**

Table 7 Coating thermo-elastic noise reduction factor $LG_{0,0}/LG_{3,3}$ for finite and infinite mirror according to the mirror dimensions

It is noteworthy that for the substrate thermo-elastic noise, the reduction factors depend on frequency range (see figure 9). At low frequencies the reduction factors are close to 1 (Table 7). From 500 to 10000 Hz, the reduction factor tends to increase up to 2.

ii. Comparison between substrates

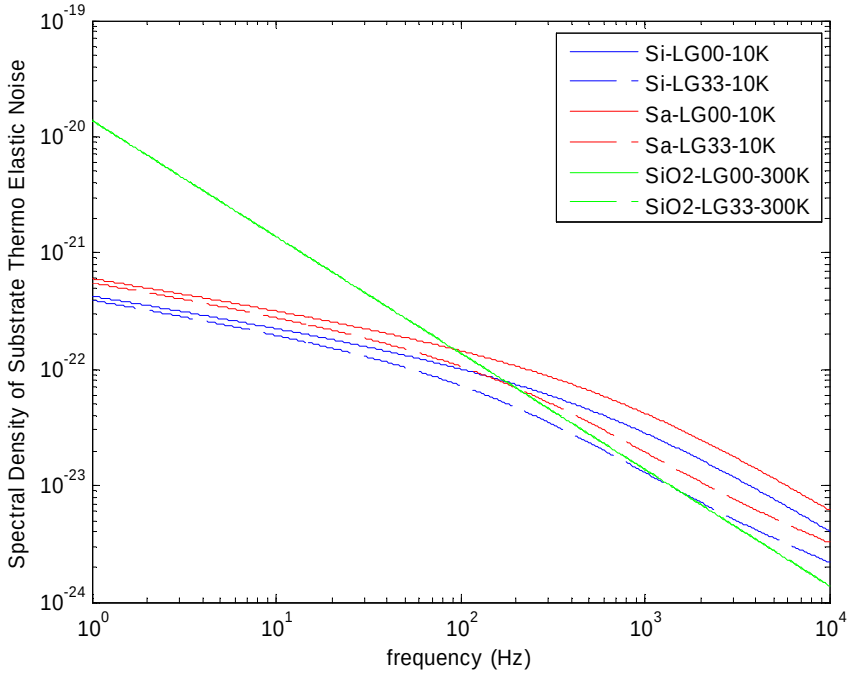

Figure 9 Substrate thermo-elastic noise for different substrates (silica at 300K, Silica at 10K and Sapphire at 10K) for a finite mirror with 35 cm diameter and 20 cm thickness

Figure 9 shows the noise spectral density curves of a finite mirror (configuration (b) for Advanced Virgo) for the three substrates. At low temperature, the adiabatic assumption fails, therefore for silicon and sapphire substrates, the formula have been revised [13]. For silica substrate at 300K the formula commonly employed has been used [14]. At low frequencies the silicon substrates gives the best sensitivity, however, at higher frequencies (> 100 Hz) silica behaves as well as silicon $LG_{3,3}$.

5. Summary

Thermal noise	Best configuration	Comments
Coating Brownian noise	Sapphire @ 10K	Sapphire is the substrate that offers the best coating thermal noise sensitivity. As of mirror dimensions, for h>10 cm there is no difference between finite and infinite mirror sensitivity. The reduction factor is close to 1.7 for a finite mirror.
Substrate Brownian noise	Silicon @ 10K	Silicon is a good substrate candidate: substrate Brownian noise is largely reduced compared to sapphire and silica substrates. Independently of the dimension of the mirror, $LG_{3,3}$ reduces the noise by a factor 2 compared to $LG_{0,0}$.
Coating thermo-elastic noise		Formulas under investigation.
Substrate thermo-elastic noise	Silicon @ 10K	The silicon substrate offers the lowest thermo-elastic noise. A reduction of the thermal noise is confirmed when using $LG_{3,3}$. The reduction factors for silicon substrate evolve with frequency from about 1.1 at low frequency to about 1.8 at high frequencies.

Table 8 Summary of the results for each thermal noise taken in account in this study

Table 8 summarizes the results obtained for the four thermal noise contributions. The previous analysis presented in the preceding section suggests that $LG_{3,3}$ gives better results than both $LG_{0,0}$ and $LG_{5,5}$. In fact, the coating dominates the thermal noise in the mirror, and the computations show that there is no significant improvement from $LG_{3,3}$ to

$LG_{5,5}$. (even if $LG_{5,5}$ is slightly better than $LG_{3,3}$ for substrate thermal noise, there is no interest in using higher order Laguerre-Gauss modes that do not compensate the coating thermal noise more than $LG_{3,3}$).

For what concerns the coating-related noise, sapphire appears to be the best material. As for the substrate thermal noise, silicon shows the best results. However, currently the limiting noise is the coating Brownian noise if we focus on the sensitivity curves of Advanced Virgo and ET (see figure 1). Therefore, our conclusion is that the best solution to decrease total thermal noise would be a sapphire-substrate mirror illuminated by a $LG_{3,3}$ beam profile. Nevertheless, silicon is not excluded because it benefits from the investments made by the microelectronics industry in order to get larger and better silicon crystals.

IV. TOTAL THERMAL NOISE

This fourth part studies the effects of a $LG_{3,3}$ beam profile for three different actual cases: Advanced Virgo, ET design at high frequencies and ET design at low frequencies.

1. Advanced Virgo

Advanced Virgo is a Michelson interferometer having an arm length of 3 km, and operating at a wavelength of 1064 nm. The design plans to use fused-silica mirrors with a diameter of 35 cm and a thickness of 20 cm [15]. The total thermal noise is computed taking into account two input mirrors and two end mirrors. The input mirrors have a coating of 6 doublets, giving a transmission of 0.7%. The end mirrors have a coating of 17 doublets, giving 6 ppm transmission.

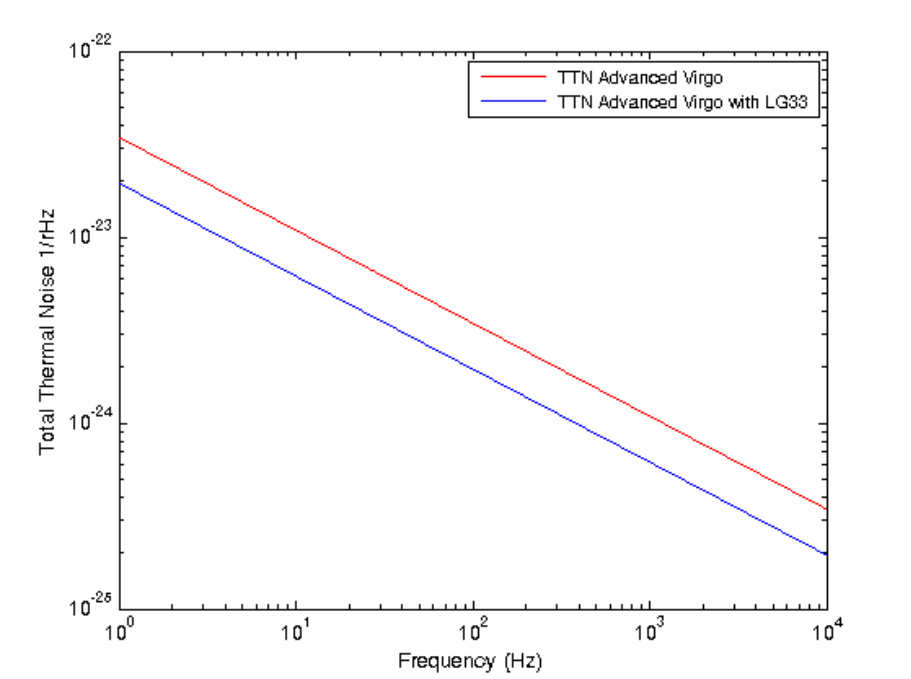

Figure 10 Comparison of total thermal noise for Advanced Virgo design with a $LG_{0,0}$ beam and a $LG_{3,3}$ beam.

Figure 10 plots the total thermal noise of Advanced Virgo design, computed for a $LG_{0,0}$ beam and a $LG_{3,3}$ beam between 1 Hz and 10 kHz. The total thermal noise for advanced Virgo when using a $LG_{3,3}$ profile is significantly reduced by a factor 1.76, which is consistent with the analysis presented in [16].

2. E.T. design at high frequencies

One of the possible designs for ET makes use of the so-called xylophone configuration, i.e., two co-located interferometers, one for detection at high-frequencies (HF) to be operated at room temperature, the other for detection at low frequencies (LF) to be operated at cryogenic temperatures[6]. In [6], the arm length is 10 km, and the laser wavelength is 1064 nm. The test masses are fused silica mirrors having a diameter of 62 cm and a thickness of 30 cm. The coating is a stack of SiO_2 and $Ti:Ta_2O_5$. Mechanical losses are $0.5\ 10^{-4}$ and $2\ 10^{-4}$ for the low refractive index thin film and high refractive index thin film respectively. The coating has the configuration HL(17)HLL in order to get the same transmission as the Advanced Virgo design (i.e. 6 ppm).

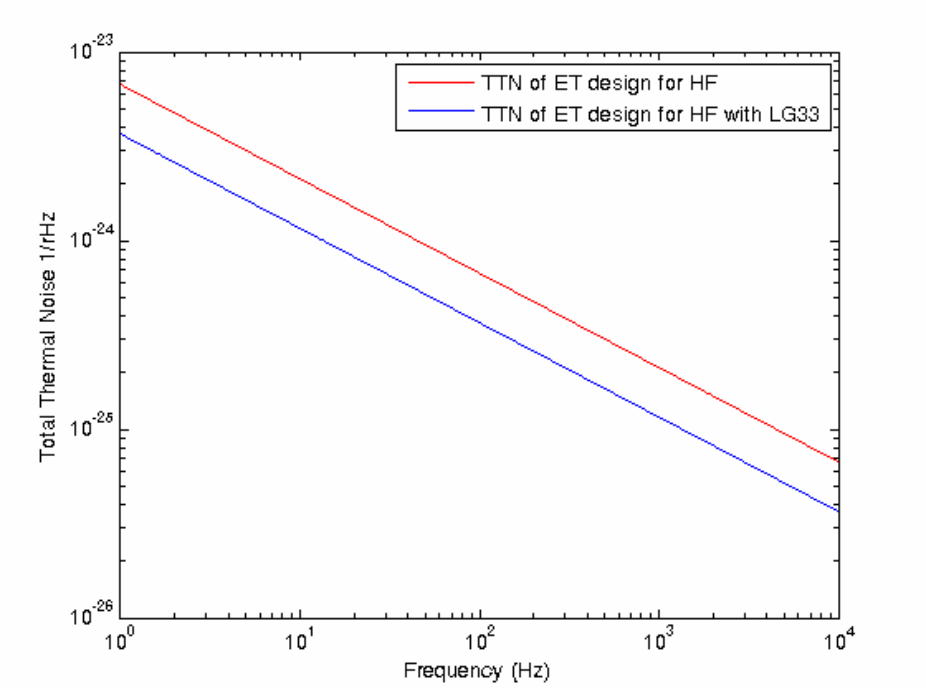

Figure 11 Comparison of total thermal noise for ET at high frequencies with a $LG_{0,0}$ and a $LG_{3,3}$ beam profile

Figure 11 shows the total thermal noise for the high-frequency interferometer of ET with a $LG_{0,0}$ and a $LG_{3,3}$ beam. The use of $LG_{3,3}$ significantly reduces the total thermal noise by a factor 1.83.

3. E.T design at low frequencies

For low frequencies, we considered the same design as in [6]. The arm length is 10 km as for the high-frequency interferometer. In contrast to the latter, we consider a substrate made of silicon, with a diameter of 62 cm and a thickness of 30 cm. The silicon has good mechanical, optical and thermal properties at cryogenic temperature that will permit to reach this kind of sensitivity. We chose a working temperature of 10K and a working wavelength of 1550 nm in order to get the accepted transmissions for input and end mirrors.

In order to attain the requested transmissions on the input mirror the number of doublet grows up to 8 (compared to 6 for the silica substrate), on the end mirror 19 doublets are required.

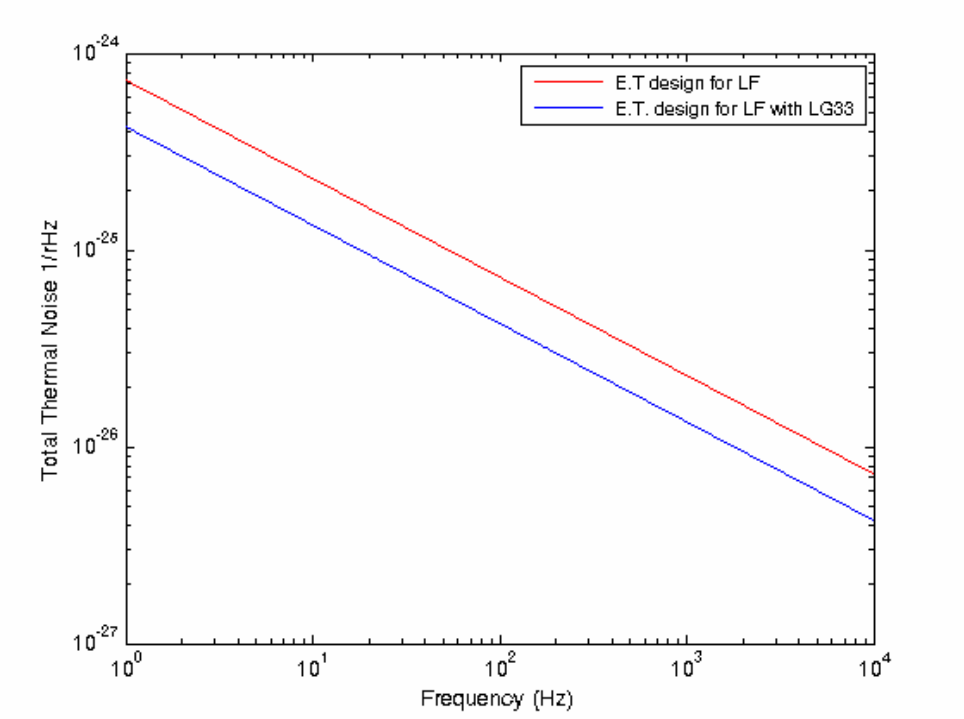

Figure 12 Comparison of total thermal noise for ET at low frequencies with a $LG_{0,0}$ and a $LG_{3,3}$ beam profile.

Figure 12 shows the total thermal noise for the low-frequency interferometer of ET with a $LG_{0,0}$ and a $LG_{3,3}$ beam. Again the use of $LG_{3,3}$ significantly reduces the total thermal noise by a factor 1.72.

4. Conclusion

These three case studies highlight the opportunity of using high-order LG beam profiles to reduce the thermal noise of future gravitational wave detectors (Advanced Virgo and ET). Table 9 summarizes the expected sensitivity at 1 Hz and the reduction factors for each of the three cases.

Detector	Beam profile	Sensitivity *h* (1/√Hz)	Reduction factor $LG_{0,0}$ / $LG_{3,3}$
Advanced Virgo	$LG_{0,0}$	$3.45\ 10^{-23}$	**1.76**
	$LG_{3,3}$	$1.96\ 10^{-23}$	
ET at high frequencies	$LG_{0,0}$	$6.74\ 10^{-24}$	**1.83**
	$LG_{3,3}$	$3.68\ 10^{-24}$	
ET at low frequencies	$LG_{0,0}$	$7.32\ 10^{-25}$	**1.72**
	$LG_{3,3}$	$4.25\ 10^{-25}$	

Table 9 Reduction factors for different detectors, computed for mirror sizes according to each detector design

In all considered telescopes, the use of a $LG_{3,3}$ profile appears to be a good choice in order to improve their sensitivity of future detectors. Moreover, as seen above (section III.1.i), the use of even higher orders gives no better results (indeed, the thermal noise values for $LG_{5,5}$ are discouraging).

V. GENERAL CONCLUSION

We have estimated the different contributions of LG modes on thermal noises (Brownian noise and thermo-elastic noise) applied to mirror substrate and coating; several concrete cases have been studied. Two high-order LG modes have been studied: $LG_{3,3}$ and $LG_{5,5}$. Our study is aimed at a better understanding of the effects of these modes on the effective thermal noise, compared to the fundamental mode. In general, $LG_{5,5}$ does not perform better than $LG_{3,3}$.

The analysis of several substrates (silica at 300 K, silicon at 10 K, and sapphire at 10 K) shows that there is no material which is always 'best', but the performances depend on the specific thermal noise considered. Although silicon implies a working wavelength of 1550 nm, which forces to increase the coating thickness, it is a material being actively researched in the microelectronics industry; this should make larger substrate sizes more easily available with respect to sapphire.

Thermal noise decreases with increasing mirror size (leading to an increase of the beam size): if we take for instance the coating Brownian noise, going from the Virgo configuration (35 cm diameter, 10 cm thickness) to the foreseen ET xylophone configuration (62 cm diameter, 30 cm thickness) allows for a decrease by a factor 2.5 for the fundamental mode, and 2.2 for a $LG_{3,3}$. These results are encouraging to push towards larger sizes.

Finally, consider the coating Brownian noise contribution to the sensitivity curve of Advanced Virgo (figure 1, dashed red line): at 100 Hz, where this noise dominates, the sensitivity is around $3\ 10^{-24}$ 1/sqrt(Hz). The expected thermal noise for a potential ET design (see section IV) reaches sensitivity lowers than 10^{-25} 1/sqrt(Hz) at 100 Hz. This means that the results we have obtained fulfill largely the ET target sensitivity at 100 Hz (about $2\ 10^{-25}$ 1/sqrt(Hz), see figure 1, continuous red line). Finally, for these simulations, we have assumed that ϕTa and ϕSiO_2 are respectively $2\ 10^{-4}$ and $0.5\ 10^{-4}$, even at low temperature, although the available measurements indicate higher loss angles for the coating materials at cryogenic temperatures than at room temperature [17]. However, it has been considered that coatings will be able to reach the same loss angles as current coatings at room temperature [6]. Within the limits of this assumption, we therefore conclude that, by adjusting beam shape, mirror dimensions, substrate material, and temperature, the target thermal noise sensitivity curve can be successfully attained.

VI. REFERENCES

1. Stefan Hild, Simon Chelkowski, and Andreas Freise, *Pushing towards the ET sensitivity using 'conventional' technology.* arXiv:0810.0604v2, 2008. **gr-gc**(2): p. 3.
2. Benoît Mours, Edwige Tournefier, and Jean-Yves Vinet, *Thermal noise reduction in interferometric gravitation wave antennas: using high order TEM modes.* Class Quantum Grav., 2006. **23**: p. 5777-5784.
3. Jean-Yves Vinet, *Reducing thermal effects in mirrors of advanced gravitation wave interferometric detectors.* Class Quantum Grav., 2007. **24**(15): p. 3897-3910.
4. Andreas Freise and Kenneth Strain, *Interferometer Techniques for Gravitational-Wave detection.* Living reviews in relativity, 2010. **13**(1).
5. Vinet, J.-Y., *On Special Optical Modes and Thermal Issues in Advanced Gravitational Wave Interferometric Detectors.* Living reviews in relativity, 2009 **12**(5).
6. Stefan Hild, S. Chelkowski, Andreas Freise, Janyce Franc, et al., *A xylophone configuration for a third generation gravitational wave detector.* Class Quantum Grav., 2010. **27**(1).
7. Kentaro Somiya and Kazuhiro Yamamoto, *Coating thermal noise of a finite-size cylindrical mirror.* Phys. Rev. D, 2009. **79**(10).
8. Uchiyama T., Kuroda K, and et al. , *Present status of large scale of cryogenic gravitational wave telescope.* Class.Quantum Grav., 2004. **21**: p. S1161-S1172.
9. M. A. Green and M. J. Keevers. in *Progr. in Photov. Res. and Appl.* 1995.
10. Penn S.D., Ageev A., Busby D., Harry G. , et al., *Frequency and surface dependence of the mechanical loss in fused silica.* Phys. Lett. A, 2006: p. 3-6.
11. Braginsky V.B. , Gorodetsky M. L. , and Vyatchanin S. P. , Phys. Lett. A, 2000. **271**: p. 301-307.
12. Cerdonio M., Conti L., Heidmann A., and Pinard M., *Thermoelastic effects at low temperatures and quantum limits in displacement measurements.* Physical Review D, 2001. **63**(082003).
13. Janyce Franc, Nazario Morgado, Raffaele Flaminio, Ronny Nawrodt, et al., *Mirror thermal noise in laser interferometer gravitation wave detectors operating at room and cryogenic temperature*, in *arXiv:0912.0107v1 [gr-qc]*. 2009.
14. Gorodetsky, M.L., *Thermal noises and noise compensation in high reflection multilayer coating.* Phys. Lett. A, 2008. **372**: p. 6813-6822.
15. Stefan Hild and Giovanni Losurdo, *Advanced Virgo design : comparison of the advanced virgo sensitivity from Bench 4 and GWINC (v1)*, in *VIR-055A-08*. 2008, VIRGO. p. 1-6.
16. Simon Chelkowski, Stefan Hild, and Andreas Freise, *Prospects of higher-order Laguerre-Gauss modes in future gravitational wave detectors.* Phys. Rev. D, 2009. **79**(12).
17. I. Martin, H. Armandula, N.M. C. Comtet, R. Flaminio, M. M. Fejer, et al., *Measurements of a low temperature mechanical dissipation peak in a single layer of Ta2O5 doped with TiO2.* Class Quantum Grav., 2008. **25**: p. 055005.